

Supplementary Material for Denitrification in soil as a function of oxygen supply and demand at the microscale

Lena Rohe¹, Bernd Apelt¹, Hans-Jörg Vogel¹, Reinhard Well², Gi-Mick Wu³, Steffen Schlüter¹

¹Helmholtz Centre for Environmental Research – UFZ, Department Soil System Sciences, Theodor-Lieser-5 Str. 4, 06120 Halle, Germany

²Thünen Institute of Climate Smart Agriculture, Bundesallee 65, 38116 Braunschweig, Germany

³Helmholtz Centre for Environmental Research – UFZ, PACE, Permoserstraße 15, 04318 Leipzig, Germany

Correspondence to: Lena Rohe, (lena.rohe@ufz.de)

Detailed information on pre-incubation, determination of water holding capacity and experimental set-up (Section 2: Material and Methods, 1. Incubation)

For pre-incubation the soil was loosely placed on a tray, adjusted to 50% water holding capacity (WHC) with a spray can and stored at room temperature in the dark for two weeks.

Additional soil cores with the same dimension were packed in an identical manner as described in the Material and Method section and fully saturated by immersion in a water bath for 24h. The water-holding capacity (v/v % WHC) for each soil material was determined after free drainage. These water volumes were taken as a reference to adjust the above-mentioned saturation levels (70, 83 and 95% WHC). Note that WHC values are not identical to water saturations expressed in v/v% water-filled pore space (WFPS), since 100% WHC covers a smaller volume than the total pore volume due to 1) air entrapment during full immersion in water and 2) drainage of the biggest pores in a pressure head range of -10 to 0cm in a 10cm tall, freely draining sample.

The cylindrical PVC columns containing the packed soil aggregates (698.41 cm³) were closed tightly by sealing caps at the top and bottom. The closed column was equipped with an in- and outlet to allow flushing the headspace (69.83 cm³) through steel capillaries (total volume 1.33 cm³). A maximal evaporation loss during incubation of one soil core is estimated to be around 1.22 g H₂O. A temperature sensor (PT100) was installed through the centre of the lid reaching the repacked aggregates with a depth of ca 3 cm down to assure constant temperature of 20°C during incubation.

28 Table with average data for each treatment (WFPS and aggregate size) with average values of CO₂, N₂O and (N₂O+N₂) fluxes, O₂
 29 saturation, total porosity, visible air content (ϵ_{vis}), connected air content (ϵ_{con}), anaerobic soil volume fraction (*ansvf*), simulated
 30 diffusivity (D_{sim}) and product ratio (*pr*) for soil from Gießen (GI) and Rothalmünster (RM)

31

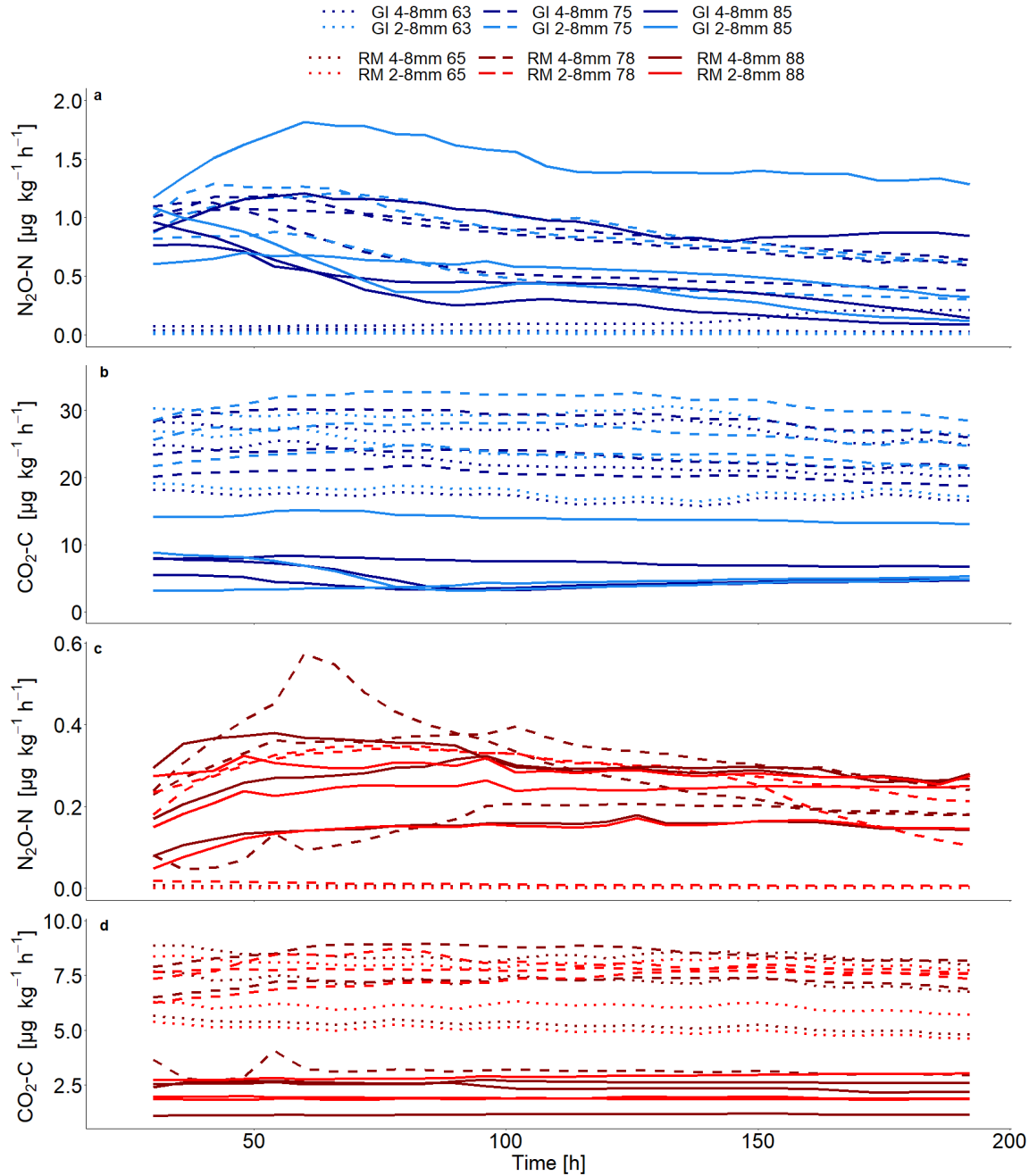
32 **Table S1: Average values for CO₂, N₂O and (N₂O+N₂) fluxes, O₂ saturation, visible air content (ϵ_{vis}), connected air content (ϵ_{con}), anaerobic soil volume fraction (*ansvf*),**
 33 **simulated diffusivity (D_{sim}) and product ratio (*pr*) [N₂O/(N₂O+N₂)]. Standard error (n=3) is shown in the brackets.**

soil	WFPS [%]	Aggregate size [mm]	CO ₂ -C [$\mu\text{g h}^{-1} \text{kg}^{-1}$]	N ₂ O-N [$\mu\text{g h}^{-1} \text{kg}^{-1}$]	(N ₂ O+N ₂)-N [$\mu\text{g h}^{-1} \text{kg}^{-1}$]	O ₂ [%air saturation]	Total porosity [-]	ϵ_{vis} [-]	ϵ_{con} [-]	<i>ansvf</i> [-]	D_{sim} [$\text{m}^2 \text{s}^{-1}$]	<i>pr</i> [-]
GI	63	2-4	23.53 (0.77)	0.01 (<0.01)	0.13 (0.08)	47.99 (1.30)	0.21 (0.03)	0.21 (0.03)	0.20 (0.03)	<0.01 (<0.01)	1.09 10 ⁻⁰⁶ (1.82 10 ⁻⁰⁸)	0.34 (0.16)
GI	63	4-8	22.10 (0.66)	0.06 (0.01)	0.13 (0.02)	55.69 (1.87)	0.20 (0.02)	0.20 (0.02)	0.20 (0.02)	<0.01 (<0.01)	1.08 10 ⁻⁰⁶ (1.56 10 ⁻⁰⁸)	0.44 (0.09)
GI	75	2-4	27.12 (0.65)	0.79 (0.11)	1.56 (0.09)	56.48 (2.50)	0.18 (0.03)	0.13 (0.03)	0.12 (0.03)	0.04 (0.02)	1.59 10 ⁻⁰⁸ (7.26 10 ⁻⁰⁹)	0.52 (0.08)
GI	75	4-8	24.10 (0.59)	0.79 (0.12)	1.18 (0.19)	61.78 (2.22)	0.19 (0.03)	0.14 (0.03)	0.11 (0.04)	0.21 (0.07)	2.76 10 ⁻⁰⁹ (2.32 10 ⁻⁰⁹)	0.68 (0.06)
GI	85	2-4	7.70 (0.59)	0.82 (0.11)	1.20 (0.28)	33.77 (1.47)	0.18 (0.03)	0.12 (0.02)	0.03 (0.03)	0.79 (0.14)	5.59 10 ⁻¹⁰ (3.36 10 ⁻¹⁰)	0.64 (0.09)
GI	85	4-8	5.52 (0.52)	0.58 (0.11)	0.94 (0.09)	39.89 (2.55)	0.20 (0.03)	0.10 (0.02)	0.01 (0.02)	0.80 (0.09)	2.00 10 ⁻¹⁰ (4.00 10 ⁻¹¹)	0.60 (0.10)
RM	65	2-4	6.36 (0.10)	<0.01 (<0.01)	NA	55.11 (2.20)	0.16 (0.03)	0.16 (0.03)	0.15 (0.03)	<0.01 (<0.01)	2.24 10 ⁻⁰⁷ (1.39 10 ⁻⁰⁸)	n.d.
RM	65	4-8	6.94 (0.12)	<0.01 (<0.01)	0.03 (0.02)	48.95 (2.56)	0.15 (0.03)	0.15 (0.03)	0.15 (0.03)	<0.01 (<0.01)	2.08 10 ⁻⁰⁷ (2.69 10 ⁻⁰⁸)	0.08 (0.04)
RM	78	2-4	7.66 (0.18)	0.19 (0.02)	0.30 (0.14)	59.16 (2.88)	0.14 (0.03)	0.10 (0.03)	0.09 (0.03)	0.08 (0.06)	1.03 10 ⁻⁰⁸ (3.65 10 ⁻⁰⁹)	0.65 (0.08)
RM	78	4-8	6.27 (0.15)	0.26 (0.04)	0.43 (0.08)	53.41 (2.60)	0.14 (0.03)	0.10 (0.03)	0.07 (0.04)	0.34 (0.22)	1.47 10 ⁻⁰⁸ (7.34 10 ⁻⁰⁹)	0.61 (0.05)
RM	88	2-4	2.22 (0.04)	0.22 (0.01)	0.37 (0.11)	22.61 (1.95)	0.10 (0.02)	0.06 (0.02)	0.03 (0.02)	0.69 (0.10)	3.27 10 ⁻¹¹ (2.02 10 ⁻¹¹)	0.64 (0.06)
RM	88	4-8	2.06 (0.05)	0.25 (0.02)	0.37 (0.08)	42.01 (2.59)	0.13 (0.03)	0.07 (0.02)	0.02 (0.01)	0.74 (0.07)	2.03 10 ⁻⁰⁹ (1.76 10 ⁻⁰⁹)	0.67 (0.04)

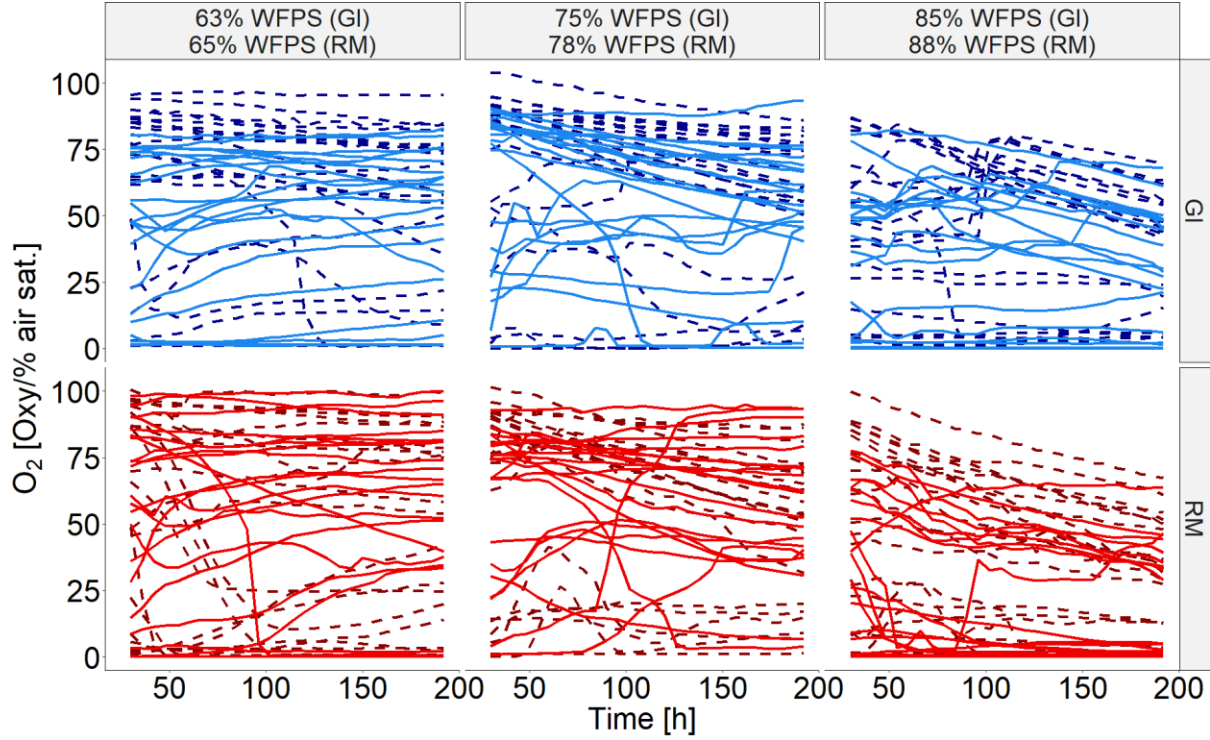
34 n.d.: not detectable; NA: not applicable

35 *N₂O* and *CO₂* fluxes and *O₂* saturation as a function of incubation time

36 *N₂O* and *CO₂* fluxes (Figure S1) and *O₂* saturation at 7 locations within the soil core (Figure S2) were
 37 measured during the incubation time of approximately 192h. In the beginning of incubation establishment
 38 of equilibrium was assumed and therefore 24h of measurements in the beginning of the incubation time
 39 were excluded.



40
 41 **Figure S1: Average *N₂O* and *CO₂* fluxes as a function of incubation time for soil from Rotthalmünster (RM) in red and**
 42 **Gießen (GI) in blue, two aggregate sizes (2-4 and 4-8 mm) and three water saturations (dotted, dashed or solid line**
 43 **depicted lowest, medium and highest water saturation, respectively) with three replicates.**



44
 45 **Figure S2: Average O₂ saturations measured by 7 sensors per soil core as a function of incubation time for soil from**
 46 **Rotthalmünster (RM) in red and Gießen (GI) in blue, two aggregate sizes (2-4 and 4-8 mm (solid and dashed lines,**
 47 **respectively)) and three water saturations with three replicates each.**

48

49 *Detailed description of calculating different pools for ¹⁵N*

50 The fraction of N in N₂O (f_{p-N_2O}) or N₂ (f_{p-N_2}) originating from ¹⁵N-labelled NO₃⁻ pool within one
 51 sample was calculated according to (Spott et al., 2006; Lewicka-Szczebak et al., 2013; Well et al., 2019)
 52 using the ¹⁵N abundance of N₂ or N₂O measured in the analyzed gas sample (a_m), in the non-labelled N₂ in
 53 technical gas (a_{bgd}), and the calculated ¹⁵N abundance of the active NO₃⁻ pool (a_p).

54
$$f_{p-N_2O} = \frac{a_m - a_{bgd}}{a_p - a_{bgd}} \quad (1)$$

55
$$f_{p-N_2} = \frac{a_m - a_{bgd}}{a_p - a_{bgd}} \quad (2)$$

56 with

57
$$a_m = \frac{{}^{29}R + 2{}^{30}R}{2(1 + {}^{29}R + {}^{30}R)} \quad (3)$$

58 and using the fraction of ³⁰N₂ in the gas sample (${}^{30}\chi_m$):

59
$$a_p = \frac{{}^{30}\chi_m - a_m \cdot a_{bgd}}{a_m - a_{bgd}} \quad (4)$$

60 This is based on the a non-random distribution of isotopes in N₂O and N₂ (Spott et al., 2006):

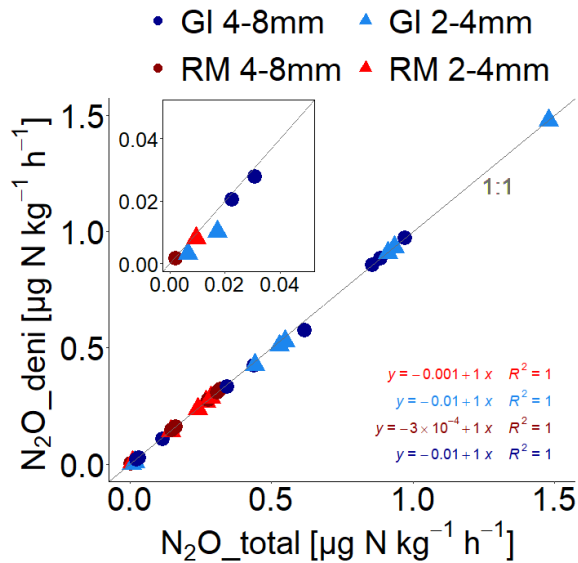
61
$${}^{30}\chi_m = \frac{{}^{30}R}{1 + {}^{29}R + {}^{30}R} \quad (5)$$

62 Thus, with $f_p\text{-N}_2\text{O}$ the N_2O flux from denitrification ($N_2\text{O_deni}$) was calculated

$$63 \quad N_2\text{O_deni} = N_2\text{O_total} * f_p\text{-N}_2\text{O} \quad (6)$$

64 The $f_p\text{-N}_2\text{O}$ was constantly near 1 for both soils, aggregate sizes, water saturations and time points of
65 sampling resulting in very similar $N_2\text{O_total}$ and $N_2\text{O_deni}$ values (Figure S3). The time resolution for
66 $N_2\text{O_total}$ was much higher than for isotopic analysis and therefore $N_2\text{O_total}$ was used to calculate $N_2\text{O}$
67 fluxes from denitrification and for statistical analysis.

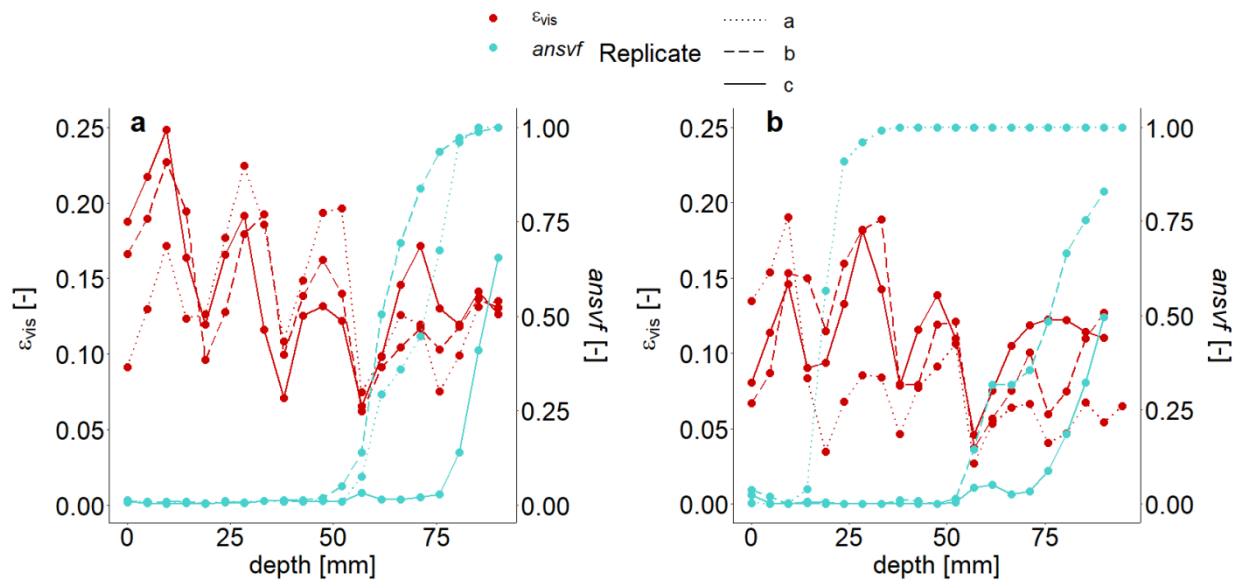
68



69

70 Figure S3: Comparison of total N_2O emissions ($N_2\text{O_total}$) captured by gas chromatography and N_2O emissions from
71 denitrification ($N_2\text{O_deni}$) from experimental treatments with soil from Rotthalmünster (RM) and Gießen (GI), two
72 aggregate sizes (2-4 and 4-8 mm) and three water saturations. Goodness of fit to the 1:1 line (gray line) is expressed as
73 slope and R^2 from linear regression.

74 *Impact of packing procedure on visible air content (ϵ_{vis}) and anaerobic soil volume fraction*
 75 *($ansvf$)*



76

77 **Figure S4: Visible air content (ϵ_{vis}) and the anaerobic soil volume fraction ($ansvf$) as a function of soil core depth for soil**
 78 **from (a) Gießen (GI) and (b) Rotthalmünster (RM). Shown here are examples of 3 replicates of repacked soil cores with**
 79 **aggregates of 4-8mm size incubated at medium water saturation of 75% with GI and 78% with RM soil. Values shown**
 80 **here for air content and anaerobic soil volume fraction are aggregated for 4.7 mm segments in depth.**

81

82 Two representative examples of one treatment were chosen to illustrate the impact of packing the soil
 83 on visible air content (ϵ_{vis}) and anaerobic soil volume fraction ($ansvf$) (large aggregates of GI soil
 84 incubated at 75% WFPS and large aggregates of RM soil incubated at 78 % WFPS) (Figure S4). During
 85 the packing procedure, intervals of 2 cm were the best option to adjust the target material-specific bulk
 86 densities and water saturations within the soil core. The average ϵ_{vis} did not differ between replicates of
 87 one treatment (Figure 4), but decreased with increasing depth of the packed soil core and was extremely
 88 reduced at the top of one packing interval (Figure S4). This varying compaction in different layers
 89 affected also the $ansvf$ of each repacked core (Figure S4). The $ansvf$ dramatically increased in layers,
 90 where lowest ϵ_{vis} was observed. In some cases, the $ansvf$ even reached 1, i.e. complete exclusion from
 91 connected air-filled pores.

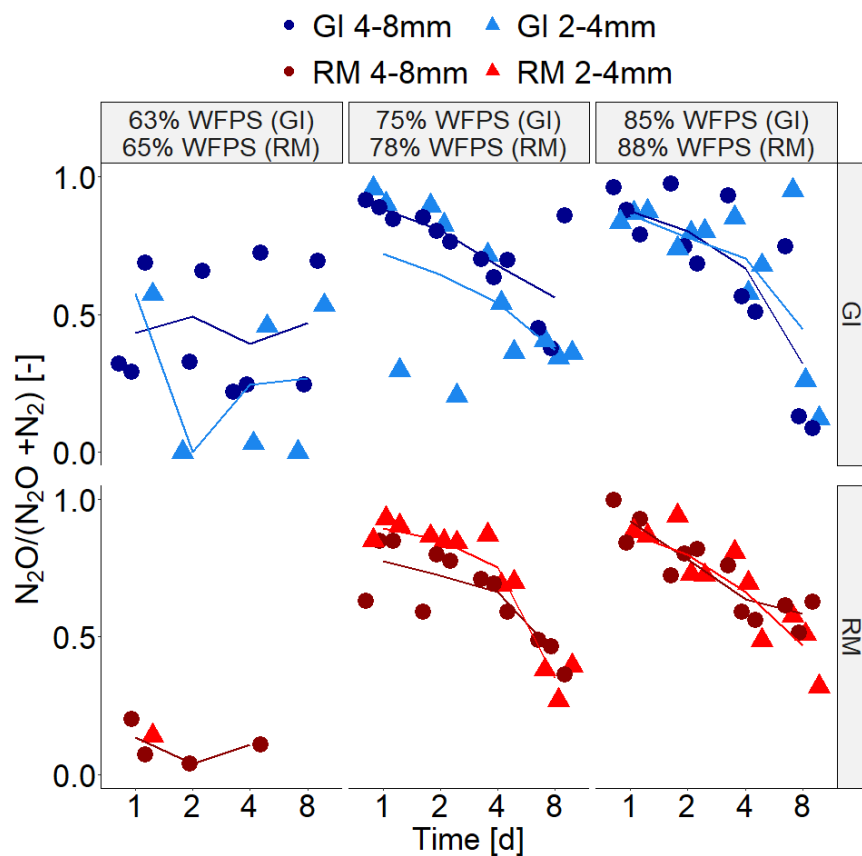
92

93 *Detailed information on simulated diffusivity (D_{sim})*

94 Diffusivity was simulated for individual aggregates as well as for the entire soil core (bulk diffusivity)
 95 directly on segmented X-ray CT data on a workstation with Intel® Xeon® CPUs (E7-8867v4, 2.46Hz, 36
 96 cores) and 6.1TB RAM by solving the Laplace equation with the DiffuDict module in the GeoDict 2019

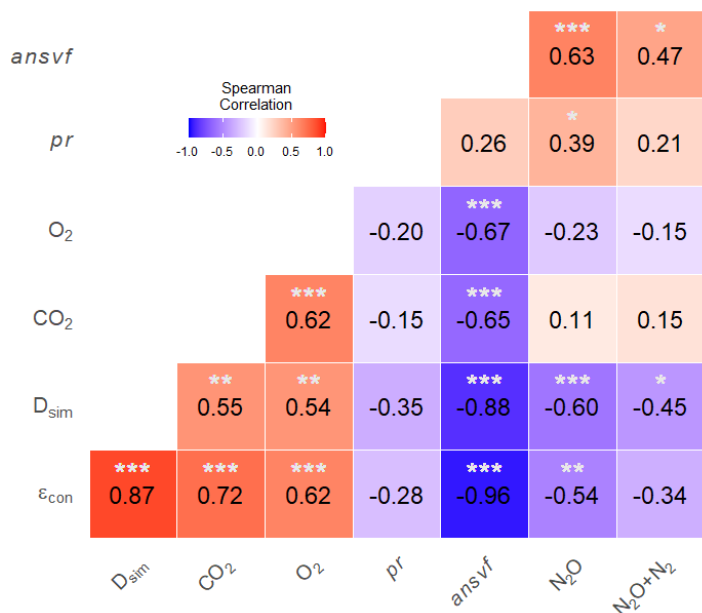
97 Software (Math2Market GmbH, Kaiserslautern, Germany). A hierarchical approach was used to estimate
98 the effective diffusivity of the wet soil matrix by simulating Laplace diffusion on cubes contained in
99 individual soil aggregates with the Explicit Jump solver assuming free diffusion in the visible pore space,
100 a completely impermeable background and symmetric boundary condition on all sides (Wiegmann and
101 Zemitis, 2006; Wiegmann and Bube, 2000). The resulting effective diffusion coefficient is expressed as a
102 percentage of the diffusion coefficient in the free fluid and was in the range of $6.6 \cdot 10^{-4} \pm 3.7 \cdot 10^{-4}\%$ and 2.4
103 $10^{-2} \pm 1.3 \cdot 10^{-2}\%$ for wet aggregates of RM and GI soil, respectively. For the soil cores with <70% WFPS
104 the visible pore space in the high-resolution aggregate images is assumed to be air-filled, whereas for soil
105 cores with $\geq 75\%$ WFPS it is assumed to be water-filled, which is justified by the fact that 1) the air-filled
106 porosity at <70% WFPS in individual aggregates (RM: 17.6%, GI: 23.1%) exceeds the visible pore space
107 in low-resolution soil core images (RM: 15.8%, GI: 20.6%) and 2) that in contrast to the higher moisture
108 levels no free water could be identified at the column scale with air-filled porosity at <70% WFPS. Thus,
109 the effective diffusion coefficient for soil matrix is determined with respect to the oxygen diffusion
110 coefficient (D_{O_2}) at 2% O_2 in pure air ($2.03 \cdot 10^{-5} \text{ m}^2 \text{ s}^{-1}$) and in pure water ($1.97 \cdot 10^{-9} \text{ m}^2 \text{ s}^{-1}$) at 20°C ,
111 respectively (<http://compost.css.cornell.edu/oxygen/oxygen.diff.air.html>).

112 Another series of diffusion experiments was modeled with the Explicit Jump solver on the entire soil
113 cores ($1550 \times 1550 \times [1500-1600]$ voxels) with the effective diffusion coefficient of the soil matrix taken
114 from aggregate simulations, an impermeable exterior, impermeable mineral grains (GI only) and the
115 diffusion coefficient of oxygen in air and water ($\geq 70\%$ WFPS only) in the respective material classes. In
116 order to save memory, periodic boundary conditions were assumed on all sides. This is irrelevant for
117 lateral boundaries as they are blocked by the impermeable exterior anyway, but may lead to a lower
118 effective diffusion coefficient, since the spatial distribution of materials at the top and bottom of the
119 domain do not match, which imposes an additional diffusion barrier. The reduction by this discontinuity
120 was in the range of $5.1 \cdot 10^{-9}$ to $6.7 \cdot 10^{-8} \text{ m}^2 \text{ s}^{-1}$ in small test images (500^3 voxels) from all soil materials and
121 saturations.

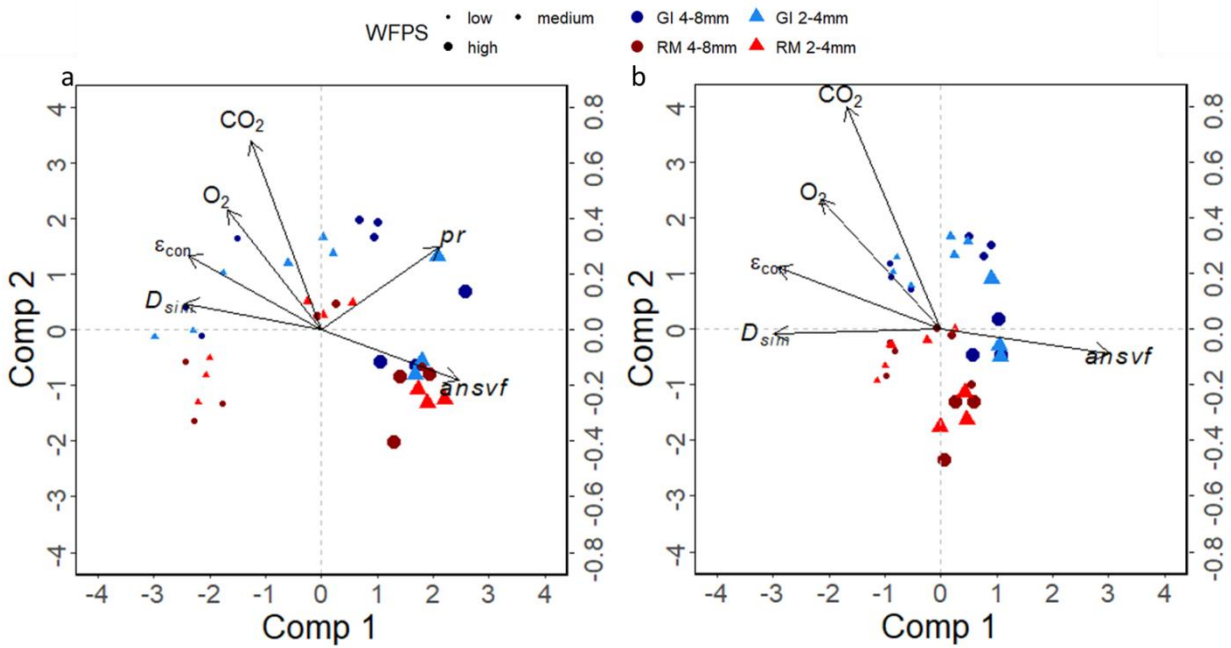


123
 124 **Figure S5: Product ratio (*pr*) [$N_2O/(N_2O+N_2)$] as a function of time for soil from Gießen (GI) in blue and Rothalmünster**
 125 **(RM) in red with aggregates of 2-4mm and 4-8mm size incubated at three water saturations. The lines connect the**
 126 **average values of three replicates (large and small aggregates, respectively).**
 127

128 *Correlation matrix*



129
 130 **Figure S6: Correlation matrix of Spearman’s rank correlation showing coefficients (R) between two measured**
 131 **variables (N_2O , (N_2O+N_2) or CO_2 fluxes, anaerobic soil volume fraction ($ansvf$), product ratio (pr), O_2 saturation (O_2),**
 132 **simulated diffusivity (D_{sim}) or connected air content (ϵ_{con}) in one cell with pairwise deletion of missing values. Asterisks**
 133 **indicate the statistical significance with significance levels of * $p \leq 0.05$, ** $p \leq 0.005$, *** $p \leq 0.001$ for adjusted p-values**
 134 **according to the method of Benjamini and Hochberg (1995). Color scheme indicate low (light colors) or strong (intensive**
 135 **colors) correlation as well as positive (red) or negative (blue) correlation.**



137
 138 **Figure S7: Biplot of the PLSR results for response variables N_2O (a) and (N_2O+N_2) fluxes (b) showing x-scores and x-**
 139 **loadings of two components (Comp 1 and Comp2). The x- and y- axis represent values of the scores for soil from Gießen**
 140 **(GI) in blue and Rotthalmünster (RM) in red with aggregates of 2-4mm (triangles) and 4-8mm size (circles) incubated at**
 141 **three water saturations depicted by the size of symbols. The second y-axis represents values for the loadings (predictors**
 142 **and arrows) to show the influence of variables on the components.**

143
 144 The regression equations with R^2 values and a confidence interval of 95% in square brackets resulting
 145 from PLSR with CO_2 , (pr) and $ansvf$ as explanatory variables to predict N_2O or (N_2O+N_2) fluxes of the
 146 present study for data after log- or logit transformation:

147 $\log(N_2O) =$
 148 $0.17 \log(CO_2) + 0.08 \text{logit}(ansvf) + 0.13 pr - 0.08 \log(D_{sim}) -$
 149 $0.03 \text{ connected air content} + 0.03 O_2; R^2 = 0.71 [0.51-0.84]$ (7)

150 $\log(N_2O + N_2) =$
 151 $0.33 \log(CO_2) + 0.18 \text{logit}(ansvf) - 0.18 \log(D_{sim}) -$
 152 $0.10 \text{ connected air content} + 0.05 O_2 ; R^2 = 0.79 [0.64-0.89]$ (8)

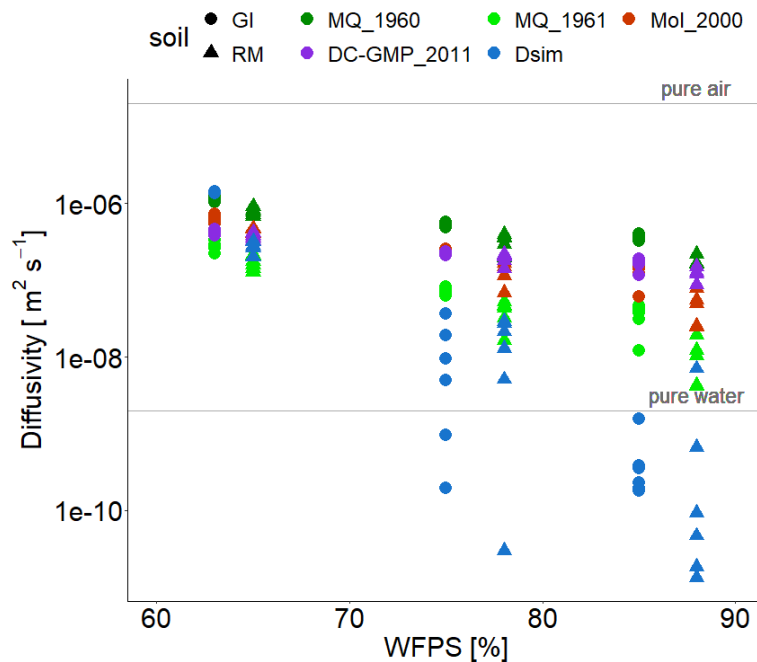
153 The regression equations with R^2 values and a confidence interval of 95% in square brackets resulting
 154 from PLSR with CO_2 , $ansvf$ (and pr) identified as most important explanatory variables to predict N_2O or
 155 (N_2O+N_2) fluxes of the present study for data after log- or logit transformation:

156 $\log(N_2O) = 0.18 \log(CO_2) + 0.14 \text{logit}(ansvf) + 0.15 pr; R^2 = 0.71 [0.55-0.83]$ (9)

157 $\log(N_2O + N_2) = 0.35 \log(CO_2) + 0.42 \text{logit}(ansvf) ; R^2 = 0.83 [0.71-0.90]$ (10)

159 *Empirical models to calculate the diffusivity of the soil cores*

160 It is assumed, that the total porosity [Φ] was unaffected by the packing procedure, whereas the air
 161 content (ε) is expected to differ from the theoretic value due to compact regions and intervals caused by
 162 the packing (Figure S4). Following from this, the target bulk density of the repacked soil cores was used
 163 to calculate Φ (0.62 or 0.51 for GI and RM soil, respectively), while CT-derived ε was used. This enabled
 164 to calculate diffusivity based on the frequently used model of Millington and Quirk (1960), Millington
 165 and Quirk (1961), Moldrup et al. (2000) and also according to the model of Deepagoda et al. (2011)
 166 (Figure S6). As expected, diffusivity from these models has a lower explanatory power for N_2O and
 167 (N_2O+N_2) release compared to D_{sim} of the present study (3D simulation) (Table S2). Higher diffusivities
 168 for treatments $\geq 75\%$ WFPS from empirical models (D_{emp}) compared to D_{sim} result from heterogeneities in
 169 compaction of the repacked soil core as described earlier (Figure S8, Figure S4), while empirical models
 170 were developed for natural soils that very likely possess higher air continuity at low air content. These
 171 empirical models only take averages for porosity and water-filled pores into account (Millington and
 172 Quirk, 1961; Moldrup et al., 2000) (Figure S8, Table S2), whereas heterogeneities in compaction are
 173 explicitly considered in 3D diffusivity simulations (D_{sim}).



174
 175 **Figure S8: Simulated diffusivities (D_{sim}) of the present study and calculated diffusivities as a function of WFPS for**
 176 **both soils (RM and GI). Models used to calculate diffusivity are published by Millington and Quirk (1960) (MQ_1960),**
 177 **Millington and Quirk (1961) (MQ_1961), Moldrup et al. (2000) (Mol_2000) and Deepagoda et al. (2011) (DC_GMP_2011).**
 178 **According to the calculations of the present study diffusivity in free air (D_0) was assumed to be $2.03 \cdot 10^{-5} m^2 s^{-1}$.**

179 Table S2: Explained variability (expressed as R^2) with confidence interval of 95% in square brackets for N_2O and
 180 (N_2O+N_2) release obtained from partial least square regression (PLSR) using explanatory variables CO_2 , diffusivity (and
 181 product ratio (pr) for N_2O as response variable only). This was done to assess possibilities to substitute one of the most
 182 important explanatory variables ($ansvf$) by diffusivity. Data were pooled for both soils (RM and GI), WFPS treatments
 183 and aggregate sizes ($n= 36$). Diffusivity was obtained by 3D simulation of the present study (D_{sim}) or existing soil gas
 184 diffusivity models were used to calculate diffusivity, using total porosity (Φ) and air content (ϵ) while diffusivity in free air
 185 (D_0) is assumed to be $2.03 \cdot 10^{-5} \text{ m}^2 \text{ s}^{-1}$.

method	Equation to calculate diffusivity D_p [$\text{m}^2 \text{ s}^{-1}$]	R^2 with response variable N_2O	R^2 with response variable (N_2O+N_2)
Present study ¹	D_{sim}	0.50 [0.23-0.71]	0.67 [0.41-0.80]
Millington & Quirk (1961) ¹	$(\epsilon^{10/3}/\Phi^2) D_0$	0.39 [0.13-0.64]	0.54 [0.23-0.72]
Millington & Quirk (1960) ¹	$(\epsilon^2/\Phi^{2/3}) D_0$	0.38 [0.11-0.63]	0.50 [0.19-0.70]
Moldrup et al. (2000) ¹	$\epsilon^{1.5} (\epsilon/\Phi) D_0$	0.50 [0.20-0.71]	0.51 [0.20-0.72]
Deepagoda et al (2011) ¹	$0.1[2(\epsilon/\Phi)^3+0.04(\epsilon/\Phi)] D_0$	0.42 [0.10-0.66]	0.64 [0.40-0.79]
theoretic air content ²	ϵ_t	0.45 [0.20-0.68]	0.76 [0.57-0.86]
no diffusivity ³	-	0.42 [0.10-0.67]	0.06

186 ¹PLSR with CO_2 and diffusivity (and product ratio (pr)) as explanatory variables and N_2O or (N_2O+N_2) as response
 187 variables.

188 ²Diffusivity substituted by the theoretic air content (ϵ_t) targeted during packing in PLSR.

189 ³Diffusivity was excluded in PLSR resulting in CO_2 (and product ratio (pr)) as explanatory variable for N_2O and for
 190 (N_2O+N_2). Because CO_2 was the single explanatory variable for (N_2O+N_2) a simple linear model was used to
 191 estimate R^2 .

192

193 Calculation of anaerobic soil volume fraction ($ansvf$) by (N_2O+N_2) fluxes from oxic and anoxic 194 incubations

195 To calculate an anaerobic soil volume fraction within the soil cores ($ansvf_{cal}$) independently from the
 196 X-ray CT imaging derived $ansvf$, parallel anoxic incubations were conducted to the described oxic
 197 incubations using a different suite of larger repacked soil cores. The conditions for incubations were very
 198 similar in soil cores as described before (in the Methods section and Supplementary Material) for oxic
 199 incubation. Deviations from the experimental protocol were the dimension of the soil core (10x14.4cm),
 200 unspecific sieving (>10mm), a flow rate of 20mL/min and a target saturation of 75% WFPS for both soils
 201 (GI and RM). Soil material was obtained from the same batches that had been used for the oxic
 202 incubations. Batches consisted of approx. 2000kg sieved, homogenized and air-dried soil stored at 6°C
 203 that had been collected and prepared to allow the study of comparable soil samples in various labs during
 204 several years. After one week with oxic incubation using a technical gas (20% O_2 and 2% N_2 in pure He)
 205 the atmospheric conditions were switched to anoxic conditions (2% N_2 in pure He). N_2O and N_2 fluxes
 206 were quantified using the ^{15}N labelling approach as described before. A comparison of oxic and anoxic
 207 (N_2O+N_2) fluxes under these comparable conditions is possible because $ansvf_{cal}$ assumes that actual
 208 denitrification is linearly related to $ansvf$ and that the specific anoxic denitrification rate is homogenous,
 209 i.e. would be identical at any location within the soil.

210 The calculated $ansvf_{cal}$ derived from incubation (N_2O+N_2) fluxes with oxic ($(N_2O+N_2)_{oxic}$) and
 211 anoxic ($(N_2O+N_2)_{anoxic}$) conditions is thus (Table S3):

$$212 \quad ansvf_{cal} = \frac{(N_2O+N_2)_{oxic}}{(N_2O+N_2)_{anoxic}} \quad (11)$$

213
 214 **Table S3: Average (N_2O+N_2) fluxes with oxic conditions ($(N_2O+N_2)_{oxic}$, present study; n=3) and with anoxic**
 215 **conditions ($(N_2O+N_2)_{anoxic}$, parallel incubations, n=4) for soils from Rothalmünster (RM) and Gießen (GI). Oxic**
 216 **incubations were conducted with two aggregate sizes (2-4 and 4-8mm) at 75% WFPS (GI) or 78% WFPS (RM). Anoxic**
 217 **conditions were established after 7 days of oxic incubation. Average (N_2O+N_2) fluxes from oxic and anoxic incubations**
 218 **served to calculate the anaerobic soil volume fraction ($ansvf_{cal}$). In comparison to the $ansvf_{cal}$, $ansvf$ derived from X-Ray**
 219 **CT imaging $ansvf_{cal}$ result from the present study is also presented**

soil	WFPS	Aggregate size [mm]	$(N_2O+N_2)_{oxic}$ [$\mu\text{g N h}^{-1} \text{kg}^{-1}$] (present study)	$(N_2O+N_2)_{anoxic}$ [$\mu\text{g N h}^{-1} \text{kg}^{-1}$] (parallel incubation)	$ansvf_{cal}$	$ansvf$ (present study)
RM	75-78	2-8	0.37	1.84	0.20	0.21
GI	75	2-8	1.37	3.60	0.38	0.13

220 Table with data for each replicate with average values of CO₂, N₂O and (N₂O+N₂) fluxes, O₂ saturation, total porosity, visible air
 221 content, connected air content (ϵ_{con}), anaerobic soil volume fraction (*ansvf*), diffusivity (D_{sim}) and product ratio (*pr*)

222 Table S4: Average values of CO₂, N₂O and (N₂O+N₂) fluxes, O₂ saturation, total porosity, visible air content (ϵ_{vis}), connected air content (ϵ_{con}), anaerobic soil volume
 223 fraction (*ansvf*), diffusivity and product ratio [N₂O/(N₂O+N₂)] for the two soils (Gießen (GI) and Rotthalmünster (RM)), three water saturations and two aggregate sizes
 224 for three replicates. Standard error of the mean is shown in the brackets.

soil	WF PS[%]	Aggregate size [mm]	Replicate	CO ₂ -C [$\mu\text{g h}^{-1} \text{kg}^{-1}$] (n=28)	N ₂ O-N [$\mu\text{g h}^{-1} \text{kg}^{-1}$] (n=28)	(N ₂ O+N ₂) [$\mu\text{g N h}^{-1} \text{kg}^{-1}$] (n=3)	O ₂ [%air saturation] (n=7)	Total porosity [-]	ϵ_{vis} [-]	ϵ_{con} [-]	<i>ansvf</i> [-]	D_{sim} [m ² s ⁻²]	<i>pr</i> (n= 1-3)
GI	63	2-4	a	17.85 (0.14)	0.01 (<0.01)	NA	47.19 (12.13)	0.20	0.20	0.19	0.003	1.10 10 ⁻⁰⁶	n.d.
GI	63	4-8	a	17.02 (0.12)	0.02 (<0.01)	0.10	53.79 (13.07)	0.19	0.19	0.19	0.004	1.05 10 ⁻⁰⁶	0.22 (n.d)
GI	75	2-4	a	23.23 (0.16)	0.94 (0.04)	1.39 (0.34)	46.27 (11.64)	0.18	0.13	0.12	0.037	2.89 10 ⁻⁰⁸	0.68 (0.14)
GI	75	4-8	a	20.35 (0.15)	0.89 (0.03)	1.33 (0.26)	59.24 (11.59)	0.19	0.14	0.10	0.246	7.50 10 ⁻¹⁰	0.67 (0.12)
GI	85	2-4	a	13.95 (0.11)	1.48 (0.03)	1.75 (0.17)	39.43 (9.42)	0.17	0.11	0.07	0.513	1.54 10 ⁻¹⁰	0.85 (0.06)
GI	85	4-8	a	7.39 (0.10)	0.97 (0.03)	1.10 (0.12)	39.66 (12.20)	0.18	0.08	0.02	0.824	1.40 10 ⁻¹⁰	0.88 (0.07)
GI	63	2-4	b	23.81 (0.37)	<0.01 (<0.01)	0.22 (NA)	45.32 (10.48)	0.22	0.22	0.21	0.001	1.11 10 ⁻⁰⁶	0.03 (n.d.)
GI	63	4-8	b	22.24 (0.32)	0.03 (<0.01)	0.11 (0.01)	57.38 (11.56)	0.21	0.21	0.21	0.001	1.11 10 ⁻⁰⁶	0.27 (0.03)
GI	75	2-4	b	26.83 (0.22)	0.91 (0.04)	1.60 (0.46)	62.33 (6.19)	0.18	0.13	0.12	0.068	1.49 10 ⁻⁰⁸	0.57 (0.14)
GI	75	4-8	b	23.07 (0.20)	0.86 (0.04)	1.42(0.34)	71.78 (7.66)	0.19	0.14	0.10	0.312	1.52 10 ⁻¹⁰	0.60 (0.12)
GI	85	2-4	b	4.19 (0.13)	0.55 (0.02)	1.01 (0.31)	28.45 (10.02)	0.18	0.12	<0.01	0.935	1.23 10 ⁻⁰⁹	0.54 (0.15)
GI	85	4-8	b	4.26 (0.12)	0.44 (0.03)	0.91 (0.40)	34.16 (9.45)	0.18	0.11	<0.01	0.938	1.82 10 ⁻¹⁰	0.48 (0.18)
GI	63	2-4	c	28.94 (0.24)	0.02 (0.04)	0.04 (<0.01)	51.43 (9.55)	0.21	0.21	0.20	<0.001	1.05 10 ⁻⁰⁶	0.50 (0.04)
GI	63	4-8	c	27.05 (0.20)	0.12 (0.04)	0.17 (0.04)	70.19 (6.95)	0.20	0.20	0.20	<0.001	1.08 10 ⁻⁰⁶	0.69 (0.02)
GI	75	2-4	c	31.29 (0.23)	0.53 (0.04)	1.70 (0.48)	60.83 (8.62)	0.19	0.13	0.13	0.018	3.88 10 ⁻⁰⁹	0.31 (0.05)
GI	75	4-8	c	28.88 (0.26)	0.62 (0.05)	0.80 (0.19)	54.30 (14.00)	0.19	0.14	0.13	0.063	7.38 10 ⁻⁰⁹	0.77 (0.05)
GI	85	2-4	c	4.96 (0.33)	0.44 (0.05)	0.83 (0.44)	23.67 (10.43)	0.18	0.12	<0.01	0.910	2.98 10 ⁻¹⁰	0.53 (0.21)
GI	85	4-8	c	4.90 (0.29)	0.34 (0.05)	0.80 (0.48)	45.84 (10.25)	0.23	0.12	0.02	0.629	2.75 10 ⁻¹⁰	0.43 (0.18)
RM	65	2-4	a	6.06 (0.03)	<0.01 (<0.01)	NA	68.61 (7.14)	0.15	0.15	0.14	0.004	2.51 10 ⁻⁰⁷	n.d.
RM	65	4-8	a	7.22 (0.04)	<0.01 (<0.01)	NA	35.75 (12.64)	0.16	0.16	0.15	0.005	2.47 10 ⁻⁰⁷	n.d.
RM	78	2-4	a	7.95 (0.07)	<0.01 (<0.01)	0.01 (<0.01)	63.18 (10.22)	0.14	0.11	0.10	0.004	1.66 10 ⁻⁰⁸	0.71 (0.16)
RM	78	4-8	a	3.12 (0.04)	0.16 (<0.01)	0.27 (0.06)	43.27 (11.97)	0.14	0.08	0.03	0.775	2.34 10 ⁻¹¹	0.60 (0.06)
RM	88	2-4	a	1.89 (<0.01)	0.14 (<0.01)	0.18 (0.03)	12.13 (8.11)	0.10	0.07	0.05	0.502	7.31 10 ⁻¹¹	0.78 (0.11)
RM	88	4-8	a	1.15 (<0.01)	0.15 (<0.01)	0.21 (0.02)	38.36 (11.27)	0.10	0.05	0.02	0.753	5.53 10 ⁻⁰⁹	0.70 (0.04)
RM	65	2-4	b	4.98 (0.33)	<0.01 (<0.01)	NA	48.38 (11.00)	0.17	0.17	0.16	0.003	2.10 10 ⁻⁰⁷	n.d.
RM	65	4-8	b	5.22 (0.37)	<0.01 (<0.01)	0.06	42.40 (11.85)	0.15	0.15	0.14	0.005	1.57 10 ⁻⁰⁷	0.04 (n.d.)
RM	78	2-4	b	7.32 (0.09)	0.27 (<0.01)	0.45 (0.15)	56.52 (8.62)	0.13	0.10	0.08	0.042	1.02 10 ⁻⁰⁸	0.60 (0.17)
RM	78	4-8	b	7.17 (0.04)	0.32 (<0.01)	0.49 (0.09)	69.43 (9.15)	0.14	0.11	0.09	0.193	2.13 10 ⁻⁰⁸	0.65 (0.10)
RM	88	2-4	b	1.89 (<0.01)	0.24 (<0.01)	0.37 (0.04)	28.13 (9.56)	0.09	0.07	0.01	0.856	1.04 10 ⁻¹¹	0.64 (0.07)
RM	88	4-8	b	2.42 (0.03)	0.31 (<0.01)	0.50 (0.08)	46.26 (9.60)	0.14	0.07	0.01	0.860	3.65 10 ⁻¹¹	0.63 (0.09)

RM	65	2-4	c	8.05 (0.03)	n.d.	NA	53.25 (14.68)	0.17	0.17	0.16	0.003	$2.10 \cdot 10^{-07}$	n.d.
RM	65	4-8	c	8.39 (0.04)	n.d.	NA	68.71 (15.40)	0.16	0.16	0.15	0.003	$2.19 \cdot 10^{-07}$	0.11 (n.d.)
RM	78	2-4	c	7.70(0.01)	0.29 (<0.01)	0.44 (0.10)	57.79 (6.92)	0.14	0.11	0.08	0.203	$4.00 \cdot 10^{-09}$	0.64 (0.13)
RM	78	4-8	c	8.51 (0.06)	0.31 (0.02)	0.54 (0.16)	58.57 (12.57)	0.14	0.11	0.10	0.062	$2.28 \cdot 10^{-08}$	0.57 (0.12)
RM	88	2-4	c	2.88 (0.02)	0.29 (<0.01)	0.56 (0.13)	27.69 (8.80)	0.11	0.05	0.02	0.720	$1.45 \cdot 10^{-11}$	0.51 (0.12)
RM	88	4-8	c	2.61 (<0.01)	0.28 (<0.01)	0.41 (0.05)	41.41 (9.23)	0.16	0.08	0.03	0.613	$5.19 \cdot 10^{-10}$	0.67 (0.08)

225 n.d.: not detectable; NO and N₂ concentration was below detection limit for IRMS analysis, thus calculation of *pr* was impossible. NA: not applicable

226 **References**

- 227 Benjamini, Y., and Hochberg, Y.: Controlling the False Discovery Rate: A Practical and Powerful
228 Approach to Multiple Testing, *Journal of the Royal Statistical Society. Series B (Methodological)*, 57,
229 289-300, 1995.
- 230
231 Deepagoda, T., Moldrup, P., Schjonning, P., de Jonge, L. W., Kawamoto, K., and Komatsu, T.: Density-
232 Corrected Models for Gas Diffusivity and Air Permeability in Unsaturated Soil, *Vadose Zone J.*, 10, 226-
233 238, <https://doi.org/10.2136/vzj2009.0137>, 2011.
- 234
235 Lewicka-Szczebak, D., Well, R., Giesemann, A., Rohe, L., and Wolf, U.: An enhanced technique for
236 automated determination of ^{15}N signatures of N_2 , $(\text{N}_2+\text{N}_2\text{O})$ and N_2O in gas samples, *Rapid Commun.*
237 *Mass Spec.*, 27, 1548-1558, <https://doi.org/10.1002/rcm.6605>, 2013.
- 238
239 Millington, R., and Quirk, J. P.: Permeability of porous solids, *Transactions of the Faraday Society*, 57,
240 1200-&, <https://doi.org/10.1039/tf9615701200>, 1961.
- 241
242 Millington, R. J., and Quirk, J. M.: Transport in porous media, in: F.A. Van Beren et. al (ed.), *Trans. Int.*
243 *Congr. Soil Sci.*, 7th, Madison, WI. 14–21 Aug, Elsevier, Amsterdam, 97–106, 1960.
- 244
245 Moldrup, P., Olesen, T., Gamst, J., Schjonning, P., Yamaguchi, T., and Rolston, D. E.: Predicting the gas
246 diffusion coefficient in repacked soil: Water-induced linear reduction model, *Soil Sc. Soc. Am. J.*, 64,
247 1588-1594, <https://doi.org/10.2136/sssaj2000.6451588x>, 2000.
- 248
249 Spott, O., Russow, R., Apelt, B., and Stange, C. F.: A ^{15}N -aided artificial atmosphere gas flow technique
250 for online determination of soil N_2 release using the zeolite Köstrolith SX6®, *Rapid Commun. Mass*
251 *Spec.*, 20, 3267-3274, <https://doi.org/10.1002/rcm.2722>, 2006.
- 252
253 Well, R., Burkart, S., Giesemann, A., Grosz, B., Köster, J. R., and Lewicka-Szczebak, D.: Improvement
254 of the ^{15}N gas flux method for in situ measurement of soil denitrification and its product stoichiometry,
255 *Rapid Commun. Mass Spec.*, 33, 437-448, <https://doi.org/10.1002/rcm.8363>, 2019.
- 256
257 Wiegmann, A., and Bube, K. P.: The explicit-jump immersed interface method: Finite difference methods
258 for PDEs with piecewise smooth solutions, *SIAM J. Numer. Anal.*, 37, 827-862,
259 <https://doi.org/10.1137/S0036142997328664>, 2000.
- 260
261 Wiegmann, A., and Zemitis, A.: EJ-HEAT: A fast explicit jump harmonic averaging solver for the
262 effective heat conductivity of composite materials, *Berichte des Fraunhofer ITWM*, 94, 2006.
- 263
264